Applied Physics Letters

1.9 W continuous-wave single transverse mode emission from 1060 nm edge-emitting lasers with vertically extended lasing area

Cite as: Appl. Phys. Lett. **105**, 151105 (2014); https://doi.org/10.1063/1.4898010
Submitted: 24 June 2014 • Accepted: 01 October 2014 • Published Online: 13 October 2014

M. J. Miah, T. Kettler, K. Posilovic, et al.

1.9 W continuous-wave single transverse mode emission from 1060 nm edge-emitting lasers with vertically extended lasing area

M. J. Miah,[1,a)] T. Kettler,[1,2] K. Posilovic,[1] V. P. Kalosha,[1] D. Skoczowsky,[2] R. Rosales,[1] D. Bimberg,[1,b)] J. Pohl,[3] and M. Weyers[3]
[1]*Institut für Festkörperphysik, Technische Universität Berlin, Hardenbergstr. 36, 10623 Berlin, Germany*
[2]*PBC Lasers GmbH, Hardenbergstr. 36, 10623 Berlin, Germany*
[3]*Ferdinand-Braun-Institut für Höchstfrequenztechnik, Gustav-Kirchhoff-Str. 4, 12489 Berlin, Germany*

(Received 24 June 2014; accepted 1 October 2014; published online 13 October 2014)

High-brightness edge-emitting semiconductor lasers having a vertically extended waveguide structure emitting in the 1060 nm range are investigated. Ridge waveguide (RW) lasers with 9 μm stripe width and 2.64 mm cavity length yield highest to date single transverse mode output power for RW lasers in the 1060 nm range. The lasers provide 1.9 W single transverse mode optical power under continuous-wave (cw) operation with narrow beam divergences of 9° in lateral and 14° (full width at half maximum) in vertical direction. The beam quality factor M^2 is less than 1.9 up to 1.9 W optical power. A maximum brightness of 72 $MWcm^{-2}sr^{-1}$ is obtained. 100 μm wide and 3 mm long unpassivated broad area lasers provide more than 9 W optical power in cw operation. © *2014 AIP Publishing LLC*. [http://dx.doi.org/10.1063/1.4898010]

High-power edge-emitting lasers are efficient and indispensable light sources for a wide range of scientific and commercial applications such as pump sources for solid-state lasers, frequency conversion, material processing, and medicine.[1–4] Numerous applications including welding, cutting, and drilling strictly require high brightness in addition to high output power. The development of high-power edge-emitting semiconductor lasers providing high beam quality has thus been the focus of extensive research in recent years.

The maximum extractable output power from semiconductor lasers is limited by the power density at the laser facets which can cause catastrophic optical mirror damage.[5] Vertical expansion of the optical field is an effective means of reducing the facet load and thus increasing the maximum output power. A large extension of the optical field also reduces the vertical far-field divergence, which allows the use of simpler low-cost optics for coupling into optical fibers and opens up various external cavity applications. Several approaches have already been implemented aiming to spread the field to very large spot sizes.[6–9] However, the high sensitivity of the field broadening to minor changes in the refractive index of ultra-thin active layers[6] and mode expansion layers[7–9] makes these approaches less attractive, since such small changes in the refractive index can be induced by slight epitaxial growth deviations, variations across the wafer or changes of the refractive indices due to current or temperature change during operation. Photonic band crystal (PBC) lasers containing an ultra-broad waveguide based on a one dimensional longitudinal PBC structure have been developed and employed.[10–17] They are proven to be robust against deviation of the refractive index of the quantum wells (QWs), thicknesses and compositions (i.e., refractive index) of the epitaxial layers within the laser structure.[12]

Here, we present further developments and modifications of PBC structures showing improved performance as compared to the original concept. A stack of quasi-periodic layers having alternating high and low refractive indices is incorporated in the vertical waveguide structure. The active region comprising several QWs is positioned at the top of the vertical layer stack. The vertical expansion of the optical modes and their confinement in the active region is controlled by the thicknesses and the refractive indices of the epitaxial layers in the PBC waveguide. For specially chosen thicknesses and refractive indices of the layers, an extended fundamental mode is generated. The fundamental mode is mostly confined in the active region and has a spatially modulated decaying tail outside. Expansion of the fundamental mode across the thick waveguide results in a narrow vertical far-field divergence. Higher order modes are shifted away from the active region towards the substrate leading to leakage of these modes into the substrate. The combination of lower confinement factor and higher leakage loss of the higher order modes favors the selection of the fundamental mode for emission.[13] Ridge waveguide (RW) PBC lasers emitting around 658 nm, 850 nm, and 980 nm have been realized.[11,17,18] In this letter, we report on PBC lasers emitting at 1060 nm providing a record single transverse mode output power, excellent beam quality, and a high brightness. The present structures have an improved mode-discriminating mechanism which arises from increased leakage of the higher order modes into the substrate. The discrimination is enhanced by an optimized doping profile in the extended waveguide.

A schematic drawing of the layer structure of a 1060-nm PBC lasers is shown in Fig. 1(a). The epitaxial layers are grown on n-doped (001) oriented GaAs substrates using metal-organic vapor phase epitaxy (MOVPE). Emission at 1060 nm wavelength is efficiently achieved with four InGaAs/GaAsP QWs. The vertical waveguide contains a layer stack of 15 AlGaAs layer pairs with alternating Al compositions. The total thickness of the vertical layer structure is about 15 μm. The thicknesses and the refractive indices of the layers are optimized to localize only the

[a)]jarez.miah@tu-berlin.de
[b)]Also at: King Abdulaziz University, Jeddah 21589, Saudi Arabia.

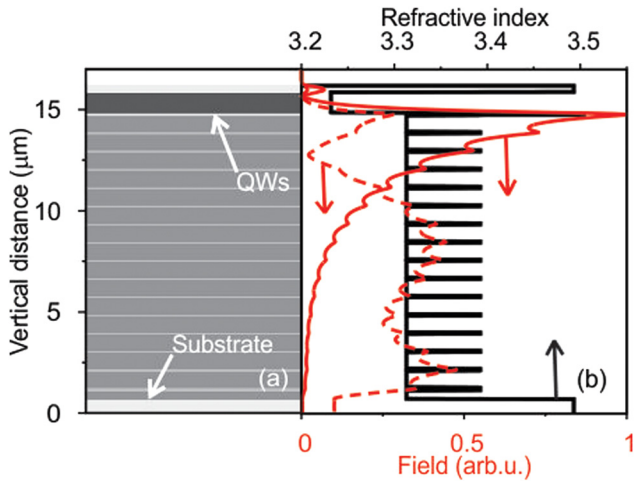

FIG. 1. (a) Schematic drawing of layer structure of the 1060-nm PBC laser and (b) refractive index profile (solid line, top axis) and modeled near-field distributions of the fundamental (solid line, bottom axis) and first higher order (dashed line, bottom axis) mode.

fundamental mode in the active region and delocalize all the other modes. The simulated field distributions of the fundamental and first higher order modes are depicted in Fig. 1(b). A graded doping profile with increasing doping concentration toward the substrate increases the free carrier absorption loss[19] of the higher order modes that have a higher intensity there than the fundamental one. Leakage of these modes into the substrate is controlled by modification of the layers closest to the substrate. Calculated optical losses, due to both free carrier absorption and leakage, and confinement factors of the first 20 modes resulting from our selected layer thicknesses and compositions are presented in Fig. 2. The fundamental mode (mode number $m = 1$) has at least one order of magnitude less loss and five time larger confinement factor than the higher order modes ($m > 1$), which gives rise to vertically single fundamental mode emission.

The structure was processed into 100 μm wide broad area and 9 μm wide RW lasers. The larger vertical mode extension also allows for a wider lateral extension and a ridge width that is larger than possible for conventional RW laser diodes, thus contributing to an increase of single

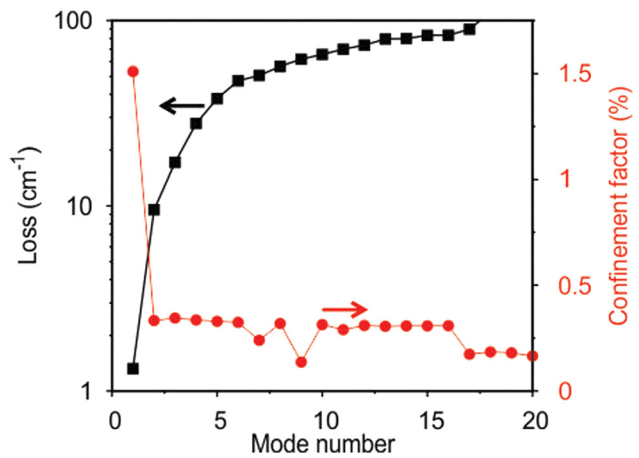

FIG. 2. Calculated combined leakage and free carrier absorption losses (square) and confinement factors (circle) of the first 20 modes in the PBC laser waveguide described in Fig. 1.

transverse mode output power. For the broad area lasers, neither facet nor passivation coatings are used. However, the facets of the 9 μm wide stripe lasers were passivated. High-reflection (HR) and antireflection (AR) coatings with 95% and 2% reflectivity, respectively, were deposited on the facets. For the characterization in continuous-wave (cw) mode, the devices are soldered p-side down on CuW heat spreader and Cu mounts.

For general device characteristics, broad area lasers having 100 μm stripe widths and different cavity lengths (L) are characterized in pulsed mode using 800 ns wide pulses at a repetition rate of 1 kHz. Figure 3 shows the cavity length dependence of differential quantum efficiency and threshold current density of the lasers at $T = 20\,^{\circ}\mathrm{C}$. The lasers exhibit a high internal efficiency η_{int} of 93% and a fairly low optical loss α_{int} of 1.3 cm^{-1}. A maximum differential quantum efficiency η_{diff} of 83% is obtained at $L = 1$ mm. The threshold modal gain Γg_0 and threshold current density at $L = \infty$ (J_∞) are deduced to be 24 cm^{-1} and 243 Acm^{-2}, respectively.

Temperature characteristics of the lasers are presented in Fig. 4. A high value of characteristic temperature $T_0 = 207$ K, within the range of 0–25 °C, ensures the good thermal stability of the devices. Above 25 °C, a still high value of $T_0 = 103$ K is obtained. Spectra of a 2 mm long broad area laser at different operating current in pulsed mode are presented in the inset. The emission wavelengths of the laser are in the range of 1060 nm.

Figure 5 shows the light-current-voltage (LIV) characteristics of a 3 mm long unpassivated broad area laser. A thermally limited maximum cw output power of 9.5 W and a maximum electrical to optical power conversion efficiency of 40% have been obtained at $T = 20\,^{\circ}\mathrm{C}$.

The LIV characteristic of a 9 μm wide and 2.64 mm long RW laser at $T = 20\,^{\circ}\mathrm{C}$ in cw mode is shown in Fig. 6. The laser has a slope efficiency of 76%, a maximum power conversion efficiency of 38%, and a maximum output power of 2.4 W, limited by thermal roll-over. Single lobe bell-shaped far-fields both in parallel (lateral) and vertical

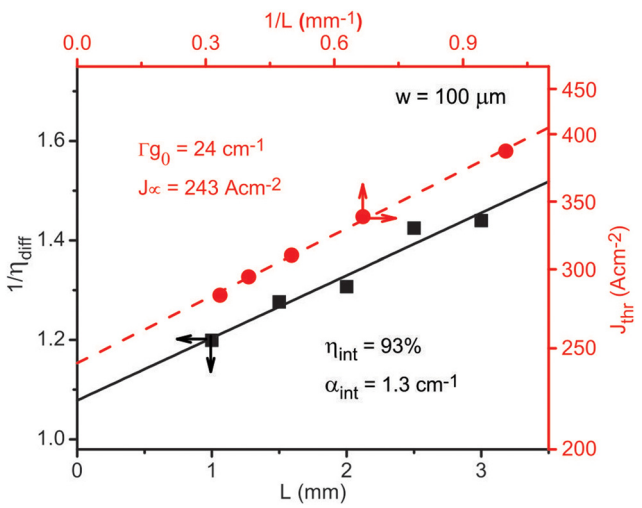

FIG. 3. Reciprocal differential quantum efficiency $1/\eta_{\mathrm{diff}}$ of 100 μm broad area PBC lasers as a function of cavity length L (square) along with linear fit (solid line) and the corresponding threshold current density J_{thr} versus inverse cavity length (circle) with linear fit (dashed line). The measurements are performed in pulsed mode (800 ns, 1 kHz) at $T = 20\,^{\circ}\mathrm{C}$.

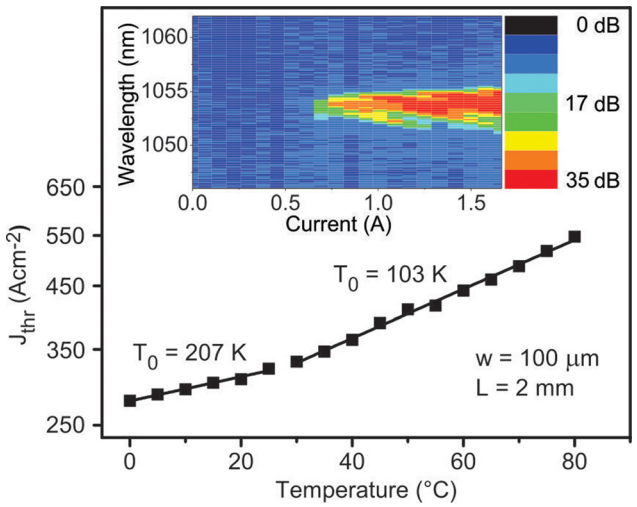

FIG. 4. Variation of threshold current density of a 100 μm wide and 2 mm long PBC laser with heat sink temperature (square). The linear fits are drawn as solid lines. The inset shows the emission wavelength of the laser vs. driving current in pulsed mode at $T = 20\,^{\circ}$C.

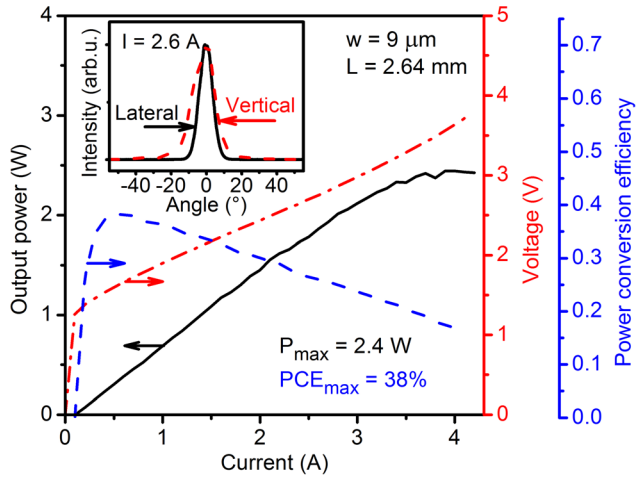

FIG. 6. Output power (solid line) in cw mode, voltage (dash-dotted line), and power conversion efficiency (dashed line) as a function of operating current of a 9 μm wide and 2.64 mm long laser at $T = 20\,^{\circ}$C. The laser is HR/AR coated. The inset shows the far-field profiles of the laser both in lateral (solid line) and vertical (dashed line) directions at $I = 2.6$ A.

directions to the p-n junctions are obtained up to 2.6 A current as depicted in the inset. No side lobes are observed. The FWHM beam divergences are 9° in lateral and 14° in vertical directions. The corresponding beam divergence angles are increased to 15° and 35° at 95% power content, respectively. The device provides a cw optical power of 1.9 W at $I = 2.6$ A, which exceeds the largest ever reported single transverse mode output power of RW laser in the 1060 nm range.[20] The lower maximum power conversion efficiencies and their strong reduction at higher currents in both broad area and RW lasers are the consequence of the relatively higher thermal and series resistances.[21] Further optimization of the optical thickness of p-doped cladding and the number of interfaces in PBC waveguide will improve both the maximum efficiency and the efficiency at intended power levels without deteriorating the optical behaviors, e.g., output power, optical loss, beam divergence.

Beam quality factors M^2, measured using the 4-σ (standard deviation) method as recommended by ISO 11146, of the laser are presented in Fig. 7. M^2 values in vertical direction vary in the range of 1.4–1.9 across the whole investigated current range. M^2 values below 1.4 are obtained in lateral direction across a wide current range up to 2.2 A. At higher current densities above 10 kA/cm^2, the lateral M^2 increases with current and reaches still low values of 1.8 at 2.6 A and 2.3 at 3.2 A. A maximum brightness of 72 MWcm^{-2}sr^{-1} is observed at 2.2 A driving current. The lasers emit a beam, whose astigmatism is almost independent on the drive current. The measured astigmatism varies only from 5 μm to 14 μm over the entire operating range.

The investigated 1060 nm PBC lasers can be widely used in applications including medical laser therapy, spectroscopy and visible light generation.[22] Due to the high brightness and excellent beam quality, they are also highly promising for more demanding present and future applications to be developed. Their brightness can be increased further by combining the single emitters coherently[23] and/or incoherently.[24] Ongoing optimization in the current PBC

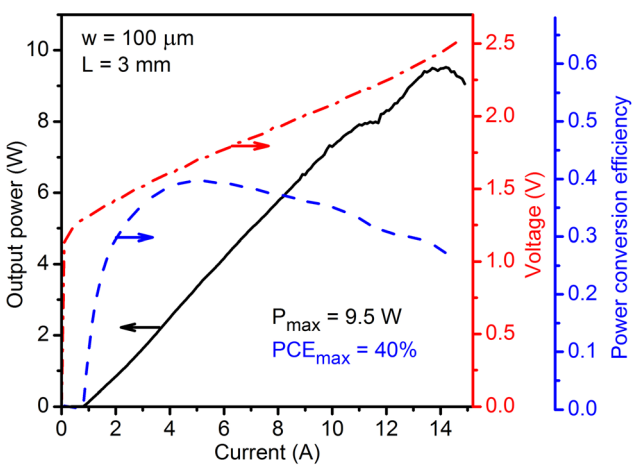

FIG. 5. Driving current dependence of optical output power (solid line), voltage (dash-dotted line) and power conversion efficiency (dashed line) of a 100 μm wide and 3 mm long broad area laser in cw-mode at $T = 20\,^{\circ}$C.

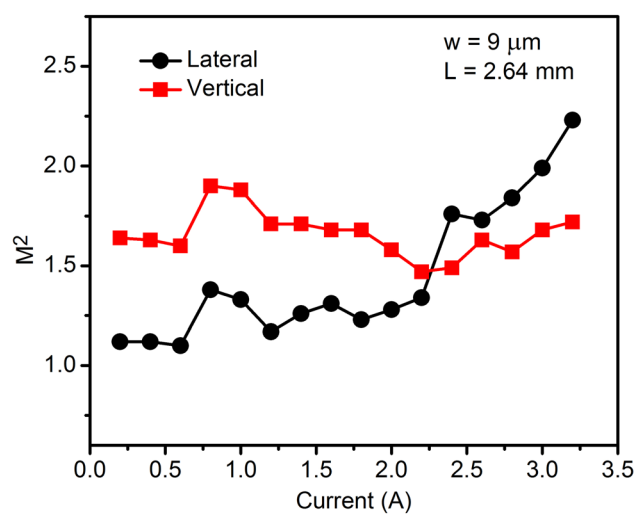

FIG. 7. Vertical (square) and lateral (circle) beam quality factor M^2 versus pump current for the laser presented in Fig. 6. The M^2 values are measured at $T = 20\,^{\circ}$C under cw operation.

structures will increase their competitiveness with presently used solutions.

In summary, we have investigated high-brightness lasers in the 1060-nm wavelength range. The lasers provide high internal quantum efficiency and low optical loss. 9 μm wide and 2.64 mm long RW lasers yield 2.4 W output power, limited by thermal effects, under cw operation. Single transverse mode emission with FWHM beam divergences of $9^\circ \times 14^\circ$ (lateral $\times$ vertical) and very low M^2 values below 1.9 are obtained at 1.9 W cw optical power. This results in a maximum brightness of 72 $MWcm^{-2}sr^{-1}$. The results demonstrate the suitability of 1060-nm PBC lasers for many cost-efficient high-brightness applications.

The authors acknowledge support of the DFG within SFB 787 and IBB within the ProFit project Bright.

[1]Y. Inoue and S. Fujikawa, IEEE J. Quantum Electron. **36**, 751 (2000).
[2]W. Schulz and R. Poprawe, IEEE J. Sel. Top. Quantum Electron. **6**, 696 (2000).
[3]U. Brauch, P. Loosen, and H. Opower, "High-power diode lasers for direct applications," in *High-Power Diode Lasers: Fundamentals, Technology, Applications*, edited by R. Diehl (Springer, Berlin, Germany, 2000).
[4]H.-G. Treusch and R. Pandey, in "High-power diode laser arrays," in *High-Power Laser Handbook*, edited by H. Injeyan and G. D. Goodno (McGraw-Hill, USA, 2011).
[5]R. W. Lambert, T. Ayling, A. F. Hendry, J. M. Carson, D. A. Barrow, S. McHendry, C. J. Scott, A. McKee, and W. Meredith, J. Lightwave Technol. **24**, 956 (2006).
[6]T. Murakami, K. Ohtaki, H. Matsubara, T. Yamawaki, H. Saito, K. Isshiki, Y. Kokubo, A. Shima, H. Kumabe, and W. Susaki, IEEE J. Quantum Electron. **QE-23**, 712 (1987).
[7]G. Lin, S.-T. Yen, C.-P. Lee, and D.-C. Liu, IEEE Photonics Technol. Lett. **8**, 1588 (1996).
[8]P. M. Smowton, G. M. Lewis, H. D. Summers, G. Berry, and C. C. Button, IEEE J. Sel. Top. Quantum Electron. **5**, 735 (1999).
[9]H. Wenzel, F. Bugge, G. Erbert, R. Hülsewede, R. Staske, and G. Tränkle, Electron. Lett. **37**, 1024 (2001).
[10]N. N. Ledentsov and V. A. Shchukin, SPIE Opt. Eng. **41**, 3193 (2002).
[11]D. Bimberg, K. Posilovic, V. Kalosha, T. Kettler, D. Seidlitz, V. A. Shchukin, N. N. Ledentsov, N. Yu. Gordeev, L. Ya. Karachinsky, I. I. Novikov, M. V. Maximov, Yu. M. Shernyakov, A. V. Chunareva, F. Bugge, and M. Weyers, Proc. SPIE **7616**, 76161I (2010).
[12]T. Kettler, K. Posilovic, L. Ya. Karachinsky, P. Ressel, A. Ginolas, J. Fricke, U. W. Pohl, V. A. Shchukin, N. N. Ledentsov, D. Bimberg, J. Jönsson, M. Weyers, G. Erbert, and G. Tränkle, IEEE J. Sel. Top. Quantum Electron. **15**, 901 (2009).
[13]V. P. Kalosha, K. Posilovic, T. Kettler, V. A. Shchukin, N. N. Ledentsov, and D. Bimberg, Semicond. Sci. Technol. **26**, 075014 (2011).
[14]M. V. Maximov, Yu. M. Shernyakov, I. I. Novikov, S. M. Kuznetsov, L. Ya. Karachinsky, N. Yu. Gordeev, V. P. Kalosha, V. A. Shchukin, and N. N. Ledentsov, IEEE J. Quantum Electron. **41**, 1341 (2005).
[15]M. V. Maximov, Yu. M. Shernyakov, I. I. Novikov, S. M. Kuznetsov, L. Ya. Karachinsky, N. Yu. Gordeev, I. P. Soshnikov, Yu. G. Musikhin, N. V. Kryzhanovskaya, A. Sharon, U. Ben-Ami, V. P. Kalosha, N. D. Zakharov, P. Werner, T. Kettler, K. Posilovic, V. A. Shchukin, N. N. Ledentsov, and D. Bimberg, Proc. SPIE **6115**, 611513 (2006).
[16]M. V. Maximov, Yu. M. Shernyakov, I. I. Novikov, L. Ya. Karachinsky, N. Yu. Gordeev, U. Ben-Ami, D. Bortman-Arbiv, A. Sharon, V. A. Shchukin, N. N. Ledentsov, T. Kettler, K. Posilovic, and D. Bimberg, IEEE J. Sel. Top. Quantum Electron. **14**, 1113 (2008).
[17]I. I. Novikov, L. Ya. Karachinsky, M. V. Maximov, Yu. M. Shernyakov, S. M. Kuznetsov, N. Yu. Gordeev, V. A. Shchukin, P. S. Kop'ev, N. N. Ledentsov, U. Ben-Ami, V. P. Kalosha, A. Sharon, T. Kettler, K. Posilovic, D. Bimberg, V. Mikhelashvili, and G. Eisenstein, Appl. Phys. Lett. **88**, 231108 (2006).
[18]T. Kettler, K. Posilovic, O. Schulz, L. Ya. Karachinsky, I. I. Novikov, Yu. M. Shernyakov, S. M. Kuznetsov, N. Yu. Gordeev, M. V. Maximov, U. Ben-Ami, A. Sharon, S. S. Mikhrin, A. R. Kovsh, V. A. Shchukin, P. S. Kop'ev, N. N. Ledentsov, U. W. Pohl, and D. Bimberg, Electron. Lett. **42**, 1157 (2006).
[19]K. A. Bulashevich, V. F. Mymrin, S. Yu. Karpov, D. M. Demidov, and A. L. Ter-Martirosyan, Semicond. Sci. Technol. **22**, 502 (2007).
[20]A. Pietrzak, H. Wenzel, P. Crump, F. Bugge, J. Fricke, M. Spreemann, G. Erbert, and G. Tränkle, IEEE J. Quantum Electron. **48**, 568 (2012).
[21]P. Crump, G. Erbert, H. Wenzel, C. Frevert, C. M. Schultz, K.-H. Hasler, R. Staske, B. Sumpf, A. Maaßdorf, F. Bugge, S. Knigge, and G. Tränkle, IEEE J. Select. Top. Quantum Electron. **19**, 1501211 (2013).
[22]M. H. Hu, H. K. Nguyen, K. Song, Y. Li, N. J. Visovsky, X. Liu, N. Nishiyama, S. Coleman, L. C. Hughes, Jr., J. Gollier, W. Miller, R. Bhat, and C.-En Zah, Proc. SPIE **6116**, 61160M-8 (2006).
[23]R. K. Huang, B. Channa, L. J. Missaggia, S. J. Augst, M. K. Connors, G. W. Turner, A. Sanchez-Rubio, J. P. Donnelly, J. L. Hostetler, C. Miester, and F. Dorsch, Conference on Lasers and Electro-Optics (CLEO) and Quantum Electronics and Laser Science (QELS), 2009.
[24]R. K. Huang, B. Chann, L. J. Missaggia, J. P. Donnelly, C. T. Harris, G. W. Turner, A. K. Goyal, T. Y. Fan, and A. Sanchez-Rubio, IEEE Photonics Technol. Lett. **19**, 209 (2007).